Enabling R-peak Detection in Wearable ECG: Combining Matched Filtering and Hilbert Transform

Theerasak Chanwimalueang, Wilhelm von Rosenberg, Danilo P. Mandic
Department of Electrical and Electronic Engineering
Imperial College London, London, United Kingdom
{tc2113, wv12, d.mandic}@ic.ac.uk

***Abstract*—Precise detection of R-peaks is a prerequisite in real-world ECG applications – this is particularly critical for wearable ECG where sensors are typically low resolution and embedded. Such recorded ECG data are typically contaminated by noise, motion artefacts, unbalanced skin-electrode impedance and other physiological signals. These affect the quality of R-peak detection and can consequently lead to failure in the evaluation of physiological functions or a misinterpretation of the state of the body, such as in monitoring stress. While numerous methods for R-peak detection are available for stationary and comparably noise-free ECG, robust DSP software for wearable devices is still emerging. To this end, a new approach which combines matched filtering and Hilbert transform is proposed. The RR-intervals and cross-correlation are used in conjunction to not only automatically locate the R-peaks but also to display the candidate ambiguous peaks via an interactive graphical user interface. The performance of the proposed approach is compared to the well-known Pan-Tompkins algorithm and is evaluated for two types of ECG databases: standard stationary data and low-SNR ECG data obtained from wearable ECG. The proposed method results in a distinctly higher positive predictivity and leads to more satisfying overall outcomes, especially for the critical call of low-SNR data.**

***Index Terms*—R-peak detection; RR-interval; ECG; QRS detection; matched filtering; Hilbert transform; wearable devices**

I. Introduction

Heart rate variability (HRV) is an important parameter for evaluating physiological mechanisms. An example of using the HRV is to measure the balance between sympathetic and parasympathetic nervous systems, where the power ratio of low and high frequencies in the HRV frequency spectrum and the sample entropy of the HRV can indicate the level of stress [1]. The electrical currents flowing through the heart muscle while triggering its contractions can be measured on the body surface. In the obtained electrocardiogram (ECG), the most prominent segment in every ECG cycle is the QRS-interval which is characterised by a sharp waveform with a high amplitude. The R-peak is the point with the maximum amplitude in this interval. The time period between two consecutive R-peaks, the RR-interval, is commonly used to calculate the heart rate and its variability over time. However, artefacts in the signal produce a number of ambiguous peaks that can potentially be the R-peak in the ECG-cycle. In stationary and wearable ECG, the causes of artefacts are mostly moving and inadequately attached electrodes [2]. Other sources of physiological signals, such as muscle contractions, also induce interfering signals. Especially when examining the HRV, the localisation of R-peaks in the ECG needs to be precise, and in case of uncertainties, they need to be examined visually by the user [2].

The extraction of R-peaks using matched filtering has been studied for many years. One approach uses the QRS complex as a pattern and searches for similarities in the ECG which [3]. To remove nonlinear and nonstationary components in noisy ECG, matched filtering was combined with an artificial neural network [4] and yielded a high accuracy when applied to the MIT/BIT arrhythmia database. In [5], [6] matched filtering is used in real-time R-peak detection while sending ECG data over a communication port. Another approach applies the Hilbert (HT) transform to find R-peaks by extracting the envelope of the ECG data [7], [8]. A narrow bandpass filter (8-20 Hz) is applied to eliminate motion artefacts and muscle activity and the derivative is utilised to remove the baseline drift [9], [10]. The approach by Pan and Tompkins (PT) [11] exhibits a high sensitivity for the R-peak detection – approximately the same as the five other algorithms compared in [12] – and its source code is publicly available. It will be used to evaluate the performance of the approach presented in this study.

Further QRS detection approaches include wavelet-based QRS detection, neural network approaches and QRS detection based on maximum a posteriori (MAP) estimation reported in [13]. However, these approaches are usually performed on ECG data acquired from stationary devices in hospitals. This study proposes a new method which combines the matched filtering and Hilbert transform (MF-HT) approaches. The former is used to find a number of potential QRS which are similar to a template QRS pattern and the exact R-peaks are located by the latter. The approach utilises a single QRS pattern manually selected once to avoid artefacts when estimating the QRS computationally. In case of multiple ambiguous R-peaks, the possible occurrences in time are limited by a dynamical time window which depends on the standard deviation of previously detected RR-intervals. Subsequently, the selection of the R-peaks is computed using the cross correlation between potential QRS and the template.

Another aspect of this work is to offer the R-peak detection software to users and researchers in medicine or psychology. The extraction and editing of the HRV from ECG data is facilitated by an interactive graphic user interface (GUI). The design of the software allows users to configure three important parameters: (i) the range of the ECG data of interest; (ii) a template QRS pattern; and (iii) the percentage error of the RR-intervals. The main feature is the automated R-peak search using the MF-HT algorithm and the simultaneous computation of the RR-intervals. The R-peak detection runs automatically until an uncertain peak is found. The program pauses and the user can select the R-peak from various choices: (i) one of the suggested peaks as identified by MF-HT; (ii) manually selecting a peak; or (iii) ignoring the detected peak. The ECG, detected R-peaks, and the calculated RR-intervals are continuously displayed graphically. Furthermore, a window in the software allows the user to enlarge an area to observe potential R-peaks in detail. The software can import .mat, .csv and .txt file formats and saves the results and configuration settings in .mat and .txt files.

978-1-4799-8058-1/15/$31.00

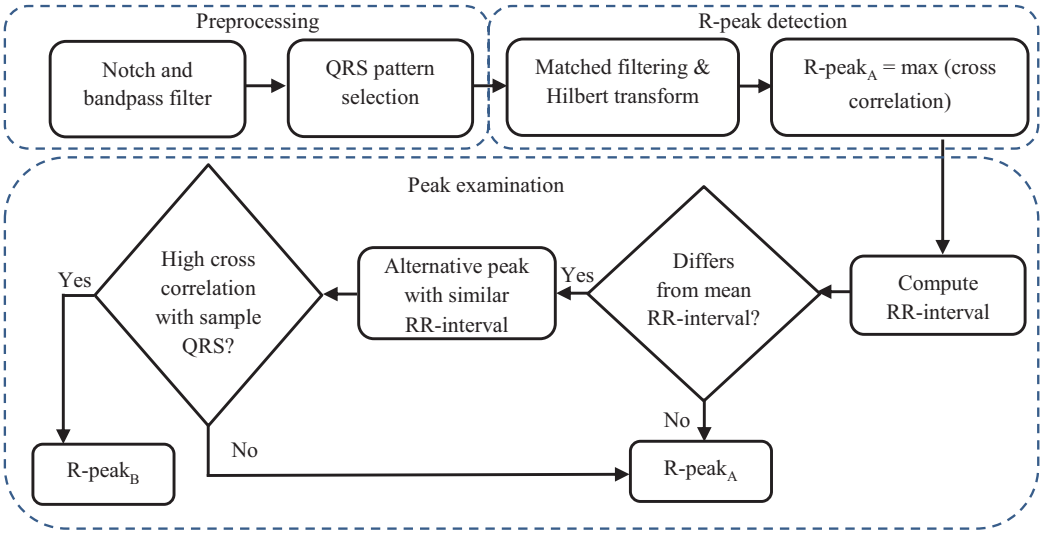

Fig. 2. The MF-HT algorithm consists of three parts: Preprocessing, R-peak detection and peak examination

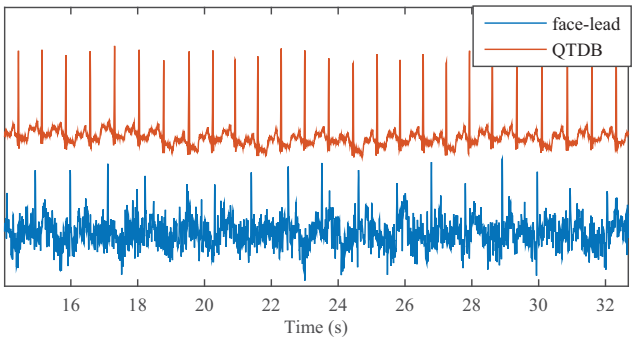

Fig. 1. The two ECG databases used to compare the algorithms. Above: QTDB with a high SNR, below: face-lead ECG with a low SNR. (The amplitudes are not to scale and the sets were recorded independently.)

II. Theory

A. Matched filtering

The idea of matched filtering is to start from a defined waveform or function and to search for a similar pattern in a time series. This is performed by taking the convolution between the conjugate of the defined mother pattern $h(k)$ and the original signal $x(n)$ with length N as shown in Eq. (1).

$$y(k) = \Sigma_{k=0}^{N-k} h(k)x(n-k) \tag{1}$$

The result of the convolution results in a high amplitude at times when the time series resembles the mother pattern and a low amplitude elsewhere. This technique is useful for locating the QRS complex in the ECG because the R-peak usually exhibits a high amplitude and the shape of QRS is unique even in noisy intervals.

B. Hilbert transform

The Hilbert transform is a tool used to extend a real function into the complex domain. The transform is shown in Eq. (2) (and in a convolution form in Eq. (3)) where $x(t)$ is a real function and the complex output of the transform is $x^h(t)$. By taking the Fourier transform shown in Eq.(4), it results in a $\pi/2$ phase-lead for a negative frequency and a $\pi/2$ phase-lag for a positive frequency as presented in Eq. (5).

$$x^h(t) = H[x(t)] = \frac{1}{\pi}\int_{-\infty}^{\infty} x(\tau)\frac{1}{t-\tau}d\tau \tag{2}$$

$$x^h(t) = \frac{1}{\pi}x(t) * \frac{1}{t} \tag{3}$$

$$X^h(j\omega) = X(j\omega)\cdot K(j\omega) \tag{4}$$

$$K(j\omega) = \begin{cases} +j, & 0 < \omega < \pi \\ -j, & -\pi < \omega < 0 \end{cases} \tag{5}$$

In an analytic form it can be written as Eq. (6) in which the Euclidean norm of the complex form is calculated from Eq.(7). The amplitude of the norm represents the local maxima or the envelope of the signal $x(t)$.

Applying the HT to $x(t)$ and computing its magitude $|s(t)|$ result in a positive envelope of the ECG data which is convenient to locate the R-peak within a specific time window.

$$s(t) = x(t) + jx^h(t) \tag{6}$$

$$|s(t)| = \sqrt{x^2(t) + x^{(h)2}(t)} \tag{7}$$

III. Method

The MF-HT algorithm is performed on shifting time windows for the length of the ECG time series. The approach can be divided into three main steps: preprocessing, R-peak detection, and peak examination as shown in Fig. 2. During the preprocessing, a notch filter at the power line frequency and a filter with a passband of 8-30 Hz, the frequency range composing the QRS [9], [10], are applied to the original ECG data. Both filters are 6th order IIR Butterworth filters. The QRS pattern QRS_{pt} is manually selected by the user within the GUI. For the R-peak detection, two time windows are created. The trend is removed in the first with its range set to 2.5 seconds which spans over more than one ECG cycle and is large

enough to estimate the local trend. A differential of consecutive samples and a median subtraction are applied to the data in the window and to QRS_{pt}. The second time window is created inside the first with a smaller duration to limit the minimum and maximum heart rate. It starts at 20% of and ends at 150% of the mean of the cumulative RR-intervals, RR_{mean}, after the last identified R-peak. The first RR-interval is set to 1 second. Therefore, the constraint for the R-peaks covers a heart rate ranging from 67% to 500% of the mean heart rate and this range is dynamically updated depending on the variation of the underlying RR-intervals. Matched filtering and Hilbert transform are applied to QRS_{pt} and the ECG data in the first window. The result from MF-HT is used to locate potential R-peaks within the second window using a minimum time threshold of $0.2 \times RR_{mean}$ to avoid physically impossible R-peaks. The length L of QRS_{pt} (in sampling points) is used to define new intervals spanning from the centre of the potential R-peaks, $QRS_{pp}(j)$, by $\pm L/2$ to both sides where j is the index of potential peaks. The root mean squares of the cross correlation between the QRS_{pt} and each $QRS_{pp}(j)$ are computed. This results in the degree of similarity $C_{rms}(j)$ for each j. The highest value of $C_{rms}(j)$, $C_{rms}(j_{max})$, is automatically chosen and selected as first R-peak, R-peak$_{\mathrm{A}}$. The RR-interval is calculated as the temporal distance between the current and the previous R-peak. The second examination becomes effective when the recently computed RR-interval differs from the defined error. This error is calculated from the standard deviation of the cumulative RR-intervals multiplied with the user-defined weight value. In the second examination, if a peak j in $QRS_{pp}(j)$ – where R-peak$_{\mathrm{A}}$ is excluded – leads to the closest RR-interval compared to the previous one and also exhibits a high $C_{rms}(j)$ among the remaining possible peaks, the peak j, R-peak$_{\mathrm{B}}$, is selected instead of the previous one.

For the length N of the ECG data $x(k)$ the MF-HT algorithm can be summarised in the following iteration steps:
While $k \leq N$

1) Create the first time window of filtered ECG data with a length of 2.5 seconds, beginning at the current R-peak.
2) Remove the local trend of the first window by taking the differential and subtracting its median from the data.
3) Define the second window ranging from $0.2 \times RR_{mean}$ to $1.5 \times RR_{mean}$ after the previous R-peak.
4) Apply matched filtering to the QRS_{pt} and the data in the first window.
5) Apply the Hilbert transform to the result from 4).
6) Find potential peaks using a minimum time threshold of $0.2 \times RR_{mean}$.
7) Create $QRS_{pp}(j)$ by expanding by $\pm L/2$ from the centre of each potential QRS to both sides.
8) Calculate cross correlation between QRS_{pt} and $QRS_{pp}(j)$ and take their root mean square resulting in $C_{rms}(j)$. $max[C_{rms}(j)]$ at j_{max} is selected to be the R-peak$_{\mathrm{A}}$ at $QRS_{pp}(j_{max})$.
9) Calculate the current RR-interval.
10) If the RR-interval is outside of the predefined error, compute RR-intervals of all j of $QRS_{pp}(j)$, where R-peak$_{\mathrm{A}}$ from 8) is excluded.
11) If the potential peak j results in the closest RR-interval value compared to the previous RR-interval and has $max[C_{rms}(j)]$ among the rest, it is selected as R-peak$_{\mathrm{B}}$ replacing R-peak$_{\mathrm{A}}$.

The GUI of the software is shown in Fig. 3.

IV. Results

The algorithm was tested on two different databases: (i) a standard database from PhysioNet [14], the QT database (QTDB) [15]; and (ii) a set of recordings partially used in [16]. The latter were recorded with a wearable device, a motorbike helmet and show a lower signal-to-noise ratio (SNR) (Fig. 1). In the first case, only the first channel was used and in the second case, one exemplary channel, a bipolar measurement between the two sides of the jaw, was selected. Out of the first 34 datasets in the QTDB, four were excluded for the following reasons: the annotations were missing for large parts of the file, the annotations were incorrect, or the annotations were inconsistent, i.e. they alternated between different parts of the QRS-intervals – in some instances the markers were closer to the Q-peaks, in other closer to the S-peaks).

After scanning the two databases for R-peaks, the detected positions in time were classified using a reference. For the QTDB, the supplied annotations were used and for the second database, a simultaneous recording of ECG obtained from the arms was utilised. Its peaks were well defined and its occurrences in time were verified visually. An R-peak was classified as correctly identified if the time difference between the R-peak in the reference and the R-peak as identified by the algorithms is smaller or equal to 20 ms which corresponds to approximately 2% of the duration of an average ECG cycle. Afterwards, the results were quantified using the parameters Sensitivity (Se) and positive predictivity ($+P$) [13]:

$$Se = \frac{TP}{TP + FN} \qquad +P = \frac{TP}{TP + FP}$$

where *TP* represents the number of correctly identified R-peaks, *FN* the number of missed R-peaks and *FP* the number of points falsely labelled as R-peaks.

However, in the case where an algorithm consistently identifies R-peaks with an offset, it can still be considered to work well as long as the offset is constant. Therefore, further parameters were considered: (i) the deviation of the RR-intervals (RRID) as obtained from the R-peak detection algorithms from the RR-intervals of the reference signal; and (ii) the analogue value for the heart rate deviation (HRD). This is quantified via the root-mean-square error of the difference between the two values at every second. The smaller the value, the more accurate was the detection of R-peaks. An example where the second method excels is the case sel808 in the QTDB. The markers for all R-peaks are positioned too early in the signal (closer to the Q-peaks). Therefore, Se and $+P$ were less than 8% for MF-HT. However, the RRID and the HRD are comparatively low – 47 ms and 2.0 bpm. While results for the HRD are more intuitive, since it is common to state the pace of the heart in beats per minute and not the average time interval between two heart beats, it is more prone to misleading results. For example, when a false R-peak was identified close to a real R-peak, the resulting heart rate will be mistakenly very high due to taking the inverse of a short time period. This explains why the values RRID and HRD in TABLE I, row MF-HT, do not show corresponding results.

TABLE I
Performance on 30 datasets from the QTDB; PT: using [11]

Algorithm	Se	+P	RRID (ms)	HRD (bpm)	Comp. Time (ms)
PT	91.2%	91.2%	1779.8	7.6	652
MF-HT	95.3%	93.5%	235.8	9.6	5347

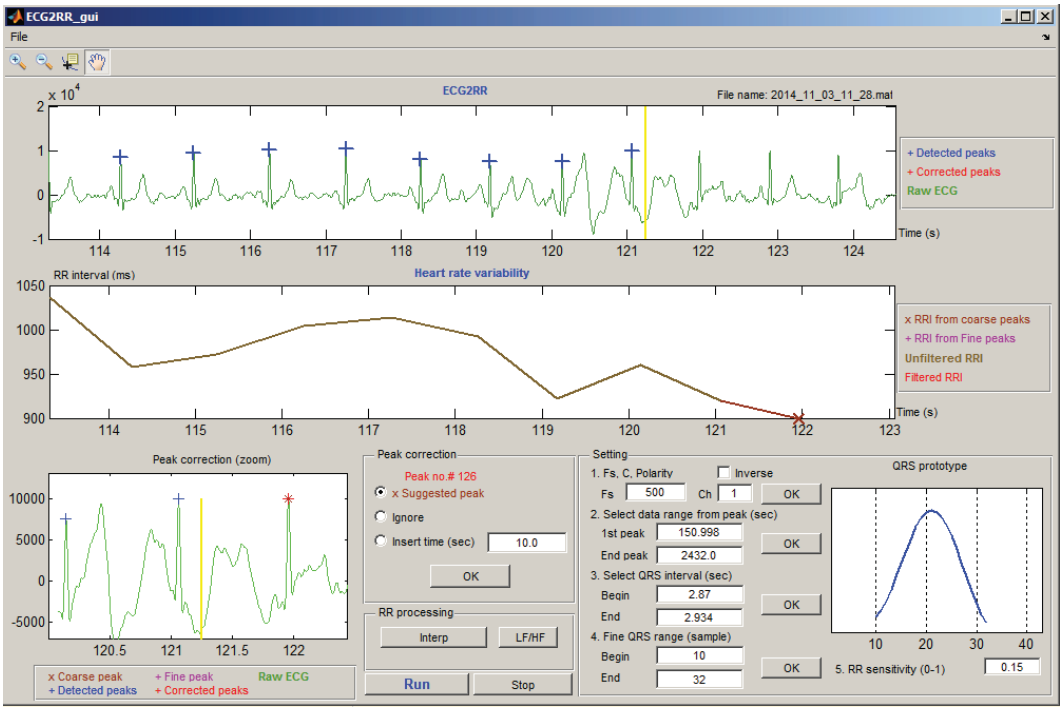

Fig. 3. Software for R-peak extraction using the MF-HT algorithm. Four windows are designed to visualise: ECG and identified R-peaks, the RR-intervals, a close-up R-peak examination with suggested choices, and the QRS pattern selection and settings.

TABLE II
PERFORMANCE ON 6 DATASETS WITH LOWER SNR; PT: USING [11]

Algorithm	Se	+P	RRID (ms)	HRD (bpm)	Comp. Time (ms)
PT	86.6%	49.6%	408.4	105.9	111
MF-HT	83.1%	86.8%	140.8	11.5	1817

The algorithm presented here was compared to a well established method by Pan and Tompkins [11]. The results for the two databases are displayed in TABLE I and TABLE II. For the QTDB, MF-HT achieved higher values for Se and $+P$ and furthermore resulted in a smaller value for RRID. Since MF-HT performed better according to the three mentioned parameters, it can be concluded that the higher value for HRD was due to an effect caused by inverting the RR-intervals to obtain the heart rate (as explained above). Examining the results for single datasets, it becomes explicit that the high values for RRID were due to a few files that are difficult to handle for the two algorithms. This is displayed in detail in Fig. 4.

The second set of ECG recordings measured with a mobile device, features a lower SNR due to electrodes placed on the head instead of the chest or the limbs. Therefore the performance of both methods was reduced. The Se of PT was a few percentage points higher than the Se of MF-HT. However, overall PT listed significantly more R-peaks that do not exist which lead to a low value for $+P$. The same behaviour is perceptible in the columns RRID and HRD: the deviation of the estimated RR-intervals and the heart rate from the real values was substantially lower for MF-HT compared to PT.

The observation that the Se and $+P$ are in general lower than in other publications (e.g. in [13]), can probably be explained by assuming that this study is more strict towards the time difference between the actual and the estimated R-peak to classify the detection as correct.

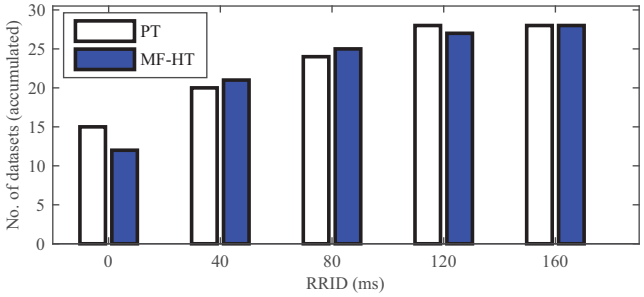

Fig. 4. QTDB: Number of datasets (out of 30) with an RRID within a specified limit. Not displayed are larger values: PT and MF-HT around 440 ms, MF-HT at 1172 ms, and PT at 9733 ms.

V. CONCLUSION

On the two examined databases, especially the one with a lower SNR, the proposed algorithm performs better than the comparative method at the expense of computation time, but is still suitable for real-time analysis. This has been achieved by combining matched filtering and Hilbert transform approaches. The cross-correlation between potential QRS and a pattern QRS and the duration of RR-intervals were utilised as criteria to select R-peaks. Furthermore, an alternative parameter to evaluate the reliability of ECG-analysing methods has been introduced.

Future work will include the verification of this result on additional standard databases and ECG data obtained from a variety of wearable devices. Moreover, the performance of MF-HT will be even higher when the GUI is used for the selection of R-peaks in critical parts of an ECG recording.

REFERENCES

[1] A. Williamon, L. Aufegger, D. Wasley, D. Looney, and D. P. Mandic, "Complexity of physiological responses decreases in high-stress musical performance," *Journal of The Royal Society Interface*, vol. 10, no. 89, 2013.

[2] M. A. Peltola, "Role of editing of R–R intervals in the analysis of heart rate variability," *Frontiers in Physiology*, vol. 3, 2012.

[3] D. Ebenezer and V. Krishnamurthy, "Wave digital matched filter for electrocardiogram preprocessing," *Journal of biomedical engineering*, vol. 15, no. 2, pp. 132–134, 1993.

[4] Q. Xue, Y. H. Hu, and W. J. Tompkins, "Neural-network-based adaptive matched filtering for QRS detection," *IEEE Transactions on Biomedical Engineering*, vol. 39, no. 4, pp. 317–329, 1992.

[5] A. Ruha, S. Sallinen, and S. Nissila, "A real-time microprocessor QRS detector system with a 1-ms timing accuracy for the measurement of ambulatory HRV," *IEEE Transactions on Biomedical Engineering*, vol. 44, no. 3, pp. 159–167, 1997.

[6] S. Dobbs, N. Schmitt, and H. Ozemek, "QRS detection by template matching using Real-Time correlation on a microcomputer," *Journal of clinical engineering*, vol. 9, no. 3, pp. 197–212, 1984.

[7] Z. Song-Kai, W. Jian-Tao, and X. Jun-Rong, "The real-time detection of QRS-complex using the envelope of ECG," *International Conference of the IEEE Engineering in Medicine and Biology Society*, vol. 1, p. 38, 1988.

[8] M. E. Nygards and L. Sornmo, "Delineation of the QRS complex using the envelope of the e.c.g." *Medical & biological engineering & computing*, vol. 21, no. 5, pp. 538–547, 1983.

[9] D. S. Benitez, P. A. Gaydecki, A. Zaidi, and A. P. Fitzpatrick, "A new QRS detection algorithm based on the hilbert transform," in *Computers in Cardiology*, 2000, pp. 379–382.

[10] D. Benitez, P. A. Gaydecki, A. Zaidi, and A. P. Fitzpatrick, "The use of the hilbert transform in ECG signal analysis." *Computers in biology and medicine*, vol. 31, no. 5, pp. 399–406, 2001.

[11] J. Pan and W. Tompkins, "A real-time QRS detection algorithm," *IEEE Transactions on Biomedical Engineering*, vol. 3, pp. 230–236, 1985.

[12] R. A. Álvarez, A. J. M. Penín, and X. A. V. Sobrino, "A comparison of three QRS detection algorithms over a public database," *Procedia Technology*, vol. 9, pp. 1159–1165, 2013.

[13] B. Köhler, C. Hennig, and R. Orglmeister, "The principles of software QRS detection," *IEEE Engineering in Medicine and Biology Magazine*, vol. 21, no. 1, pp. 42–57, 2002.

[14] A. L. Goldberger, L. A. Amaral, L. Glass, J. M. Hausdorff, P. C. Ivanov, R. G. Mark, J. E. Mietus, G. B. Moody, C. Peng, and H. E. Stanley, "Physiobank, physiotoolkit, and physionet components of a new research resource for complex physiologic signals," *Circulation*, vol. 101, no. 23, pp. e215–e220, 2000.

[15] P. Laguna, R. G. Mark, A. Goldberg, and G. B. Moody, "A database for evaluation of algorithms for measurement of QT and other waveform intervals in the ECG," in *Computers in Cardiology*, 1997, pp. 673–676.

[16] W. von Rosenberg, T. Chanwimalueang, D. Looney, and D. P. Mandic, "Vital signs from inside a helmet: A multichannel face-lead study," in *Proceedings of the IEEE International Conference on Acoustics, Speech and Signal Processing (ICASSP)*, vol. TBC, 2015, p. TBC.